# Post-print version:

## INVALIDATION OF LOW-ORDER MODELS FOR AP CONTROLLER DESIGN

F.D. Bianchi, M. Moscoso-Vásquez, P. Colmegna and R.S. Sánchez-Peña

## BibTex:

```
@Article{Bianchi2016,
    Title   = {Invalidation of low-order models for AP controller design},
    Author  = {Fernando D. Bianchi and Marcela Moscoso-Vásquez and Patricio
        Colmegna and Ricardo S. Sánchez-Peña},
    Journal = {Journal of Process Control},
    Year    = {2019},
    Number  = {},
    Pages   = {133-140},
    Volume  = {76},
    Doi     = {10.1016/j.jprocont.2019.02.004}
}
```

# Invalidation and Low-Order Model Set for Artificial Pancreas Robust Control Design

Fernando D. Bianchi[a,e], Marcela Moscoso-Vásquez[b,e], Patricio Colmegna[c,d,e], Ricardo S. Sánchez-Peña[b,e,*]

*[a]Instituto Balseiro, CNEA, Bariloche, Argentina*
*[b]Instituto Tecnológico de Buenos Aires (ITBA), Argentina*
*[c]University of Virginia (UVA), Charlottesville, USA*
*[d]University of Quilmes (UNQ), Buenos Aires, Argentina*
*[e]CONICET, Argentina*

## Abstract

The purpose of this work is to compute a Linear Parameter-Varying (LPV) model set that describes the insulin-glucose dynamics in Type 1 Diabetes (T1D). This set includes a nominal LPV model and dynamic uncertainty and is amenable to controller design. The nominal model is an LPV control-oriented model previously published by the authors that is (in)validated in this work against the UVA/Padova metabolic simulator. The result is a set of models that is used to design a switched LPV robust controller to account for nonlinearities and variations in Insulin Sensitivity ($S_I$). Closed-loop responses obtained with the robust controller and a nominal one are compared. Results illustrate the convenience of including robust strategies in designing control laws for an Artificial Pancreas (AP).

*Keywords:* Artificial Pancreas, Control-Oriented Models, Model (In)Validation, Type 1 Diabetes Mellitus, LPV Control.

## 1. Introduction

Type 1 Diabetes (T1D) is a disease characterized by the inability to produce insulin due to the destruction of the pancreatic $\beta$-cells. Although Intensive Insulin Treatment (IIT) regimens have beneficial effects on the risk of diabetes complications, they are extremely demanding for the patient and also associated with an increased risk of hypoglycemia [1]. Therefore, an Artificial Pancreas (AP) system that automatically modulates the patient's insulin infusion rate appears as a better solution to maintain his/her glucose concentration within safe limits. An AP system consists of a glucose sensor and an insulin pump both connected by a control algorithm. Subcutaneous devices are usually selected, leading to a minimally invasive AP scheme, but also, unfortunately, to a harder control problem due to the large lag times associated with glucose measurement and insulin action. Moreover, designing AP controllers is inherently challenging, because the insulin-glucose system is characterized by nonlinear time-varying dynamics and significant inter- and intrasubject variability [2].

---

*Corresponding author.
*Email addresses:* `fernando.bianchi@ib.edu.ar` (Fernando D. Bianchi), `mmoscoso@itba.edu.ar` (Marcela Moscoso-Vásquez), `pc2jx@virginia.edu` (Patricio Colmegna), `rsanchez@itba.edu.ar` (Ricardo S. Sánchez-Peña)

The AP development has been accelerated by the use of elaborated simulators, such as the UVA/Padova metabolic simulator that was accepted by the US Food and Drug Administration (FDA) in lieu of animal trials [3–5], and has been extensively used for model identification and testing of AP controllers [6–16]. The main goal of T1D simulation models is to provide a blood glucose prediction as close as possible to a real situation in order to perform *in-silico* pre-clinical tests. However, this kind of models is not generally used for controller synthesis, given its mathematical complexity. Therefore, they are usually simplified, generating the so-called *control-oriented* models. Clearly, control-oriented models have to represent the underlying dynamics, but with a simple mathematical formulation that facilitates the controller design. In addition, it is worth remarking that using complex models for synthesis does not necessarily guarantee better closed-loop performance [17].

Several control-oriented models have been introduced in the past [6, 9, 11, 13, 18], and Linear Parameter-Varying (LPV) models have been presented in previous works as a way to represent the time-varying nature of the T1D problem [19, 20]. Recently, an LPV control-oriented model, developed by the authors, has been sucessfully compared with other models using the Root Mean Square Error (RMSE) and the $\nu$-gap metric [16]. In addition, interval models have been used to describe model uncertainty for analysis and simulation purposes [21–24]. Time-varying parameters have been included in intervals to reflect how intra-patient variability propagates through the nonlinear dynamics in order to analyze the robustness of the design. Nevertheless, no uncertainty quantification has been introduced for controller synthesis using this technique.

The glucose-insulin system presents characteristics that should be tackled in a quantifiable way: nonlinear/time-varying dynamics and uncertainty, both inter- and intra-patient. Fortunately, there is a framework that deals with both problems, i.e., *robust control* accounts for parametric and dynamic uncertainty, and *LPV control* represents most nonlinear dynamics, including this problem. In both methodologies, well-known and numerically robust techniques can be applied to the analysis and synthesis stages. Within the robust control framework, controller designs that include uncertainty, although not explicitly, have used $\mathcal{H}_\infty$ optimal control that only consider time-invariant dynamics [25–27]. LPV techniques have also been applied to modeling [28] and design [11, 29–31]. Moreover, robust Model Predictive Control (MPC) controllers have been developed as well, using interval or physiology-based models [32, 33].

To obtain a model set in a robust control framework, uncertainty bounds should be computed after comparing a nominal model with experimental data. A systematic way to do this is through (in)validation techniques [34, 35]. There are no previous works in the field that have produced a model set or any uncertainty bounds in this way, for this problem.

The results presented in this work will extend the validity of a particular LPV control-oriented model to a set of models so as to represent uncertain dynamics. The model set will be obtained by means of an invalidation procedure. Here, (in)validation is refered to a technique that compares the I/O data of an *experiment*, with a given nominal model, under model uncertainty and noise bounds in order to determine if model and data are consistent. In this paper, experiments are obtained from the UVA/Padova metabolic simulator and the nominal model is the LPV description presented in [16, 36]. Both noise and uncertainty bounds are minimized so that the data could have been produced by the nominal model with uncertainty. This procedure provides a quantification of the model error with respect to this simulator and produces an LPV *model set* that is amenable to design robust controllers that take into account several sources of

uncertainty, e.g., nonlinearities and variations in Insulin Sensitivity ($S_I$).

Next section presents some background on control-oriented models and invalidation, and Section 3 describes the LPV invalidation results. Section 4 illustrates the use of the model set with the design of a switched LPV controller that is tested on the *in-silico* adult cohort of the distribution version of the UVA/Padova simulator. Conclusions and future research issues are presented in Section 5.

## 2. Background material

### 2.1. Control-oriented models

One interesting approach to obtain a personalized T1D control-oriented model is to adapt a low-order model structure based on *a priori* patient information. For example, given the patient's Total Daily Insulin (TDI), an insulin sensitivity factor can be obtained using the 1800 rule (1800/TDI) [37]. From the medical point of view, the 1800 rule indicates the maximum drop in glucose concentration, measured in mg/dl, after a 1 U injection of rapid-acting insulin. Since the work in [6], that rule has been used in several studies, both *in-silico* and clinical, to tune the gain of a Linear Time Invariant (LTI) model to a particular patient [6, 9, 11].

A good control-oriented model should have a structure that allows a well-known, reliable and numerically robust control synthesis technique to produce a controller that can be implemented in real-time. This control design method should be simple enough to allow real-time implementation, but at the same time it should have sufficient *dynamical richness* to overcome the obstacles of this particular problem: nonlinearities, time delays, inter- and intra-patient variations, among others. Good candidates for an AP controller design are LPV models or families of LPV (LTI) models, which can produce LPV or switched LPV (LTI) controllers.

Examples of LPV models that have been proposed to describe the insulin-glucose dynamics can be found in [19, 20, 38–41]. In [19] and [38], the Bergman minimal model [42] was considered and transformed into a quasi-LPV model by an appropriate choice of parameters. In [39–41], the Sorensen compartmental model [43] was linearized at different points, which were defined as the vertexes of an affine-LPV model that covers the original nonlinear one. This model was used as an uncertainty LTI model set, and an $\mathcal{H}_\infty$ controller was designed to control it, hence, the time-varying characteristics were not exploited. Finally, in [20], the Cambridge model [44] was represented with an LPV system by a particular selection of scheduling variables. The LPV system was used to obtain a robust LPV controller that was tested on different *in-silico* scenarios, showing the benefits of including uncertainty on the controller synthesis.

The control-oriented LPV model used in this work was developed by two of the authors in [16, 36]. Model identification and tuning were performed using the distribution version of the UVA/Padova metabolic simulator, around different basal operating points. Without going into greater detail, in [16, 36], a low-order LTI model was proposed, similar to the one in [6], where the input corresponds to the subcutaneous insulin infusion (in pmol/min) and the output is the glucose concentration deviation (in mg/dl):

$$G(s) = k \frac{s + z}{(s + p_1)(s + p_2)(s + p_3)} \mathrm{e}^{-15s}. \tag{1}$$

Next, the nonlinear behavior of the insulin-glucose system was described through the construction of an LPV average model (over all subjects) by making the parameter $p_1$ vary with respect to the glucose value,

keeping all the other parameters fixed ($z = 0.1501$, $p_2 = 0.0138$ and $p_3 = 0.0143$). Pole $p_1(g)$ has been approximated by a piecewise-polynomial function. The gain parameter $k$ is time-invariant, but is adjusted for each particular patient by means of his/her particular TDI. Given a subject $\#j$, the LPV model is excited with a 1 U insulin bolus and the value of $k_j$ is determined so that the glucose drop matches the 1800 rule (1800/TDI). Here, the bolus is applied at 235 mg/dl, which is the operating point where the 1800 rule is on average rendered correct for the nonlinear model [16, 36]. Therefore, an average LPV model is proposed and is then personalized through the subject's TDI, which is easily obtainable from clinical data. Below, a state-space representation of the personalized LPV model is presented:

$$\begin{aligned}
\dot{x}(t) &= A(p_1)x(t) + Bu(t) \\
y(t) &= Cx(t)
\end{aligned} \tag{2}$$

with $u$ and $y$ the insulin delivery and glucose signals, and

$$A(p_1) = \begin{bmatrix} 0 & 1 & 0 \\ 0 & 0 & 1 \\ 0 & -p_2 p_3 & -(p_2 + p_3) \end{bmatrix} + p_1 \begin{bmatrix} 0 & 0 & 0 \\ 0 & 0 & 0 \\ -p_2 p_3 & -(p_2 + p_3) & -1 \end{bmatrix}, \tag{3}$$

$$B = \begin{bmatrix} 0 & 0 & 1 \end{bmatrix}^T, \quad C = k_j \begin{bmatrix} z & 1 & 0 \end{bmatrix}.$$

Note that model (2) is affine in the parameter $p_1(g)$, which depends on the glucose level. According to the results presented in [16, 36], this LPV model has a better fit with the simulator in terms of the RMSE and the $\nu$-gap metric than others presented previously in this field. This fact indicates a potentially better closed-loop performance when designing a controller based on this model.

### 2.2. Model (in)validation

The idea behind model (in)validation[1] is to verify if a given model is consistent with an experimental data set $(u(t_k), y(t_k), \rho(t_k))$ with $k = 0, \ldots, N - 1$, where $u(t_k)$, $y(t_k)$ and $\rho(t_k)$ are the measures of the input, output and varying parameter, respectively. In order to accommodate small differences between the model output and the experimental information, the system is usually described by a set of models parameterized by a nominal model $G(\rho)$, a (dynamic) uncertainty bound $\Delta$, and an output disturbance $d$. For instance, the model set may be defined as illustrated in Figure 1, that is,

$$\mathcal{G} = \{G(\rho)(1 + W_\delta(s)\Delta), \ \Delta \in \boldsymbol{\Delta}\} \tag{4}$$

where

$$\boldsymbol{\Delta} = \{\Delta \in \mathcal{H}_\infty \ : \ ||\Delta||_\infty \le \gamma\}, \tag{5}$$

$W_\delta(s)$ is a stable transfer function specifying the uncertainty dependence on frequency, $\mathcal{H}_\infty$ is the set of stable transfer functions with suitable dimensions, and $||\Delta||_\infty = \sup_\omega |\Delta(j\omega)|$. On the other hand, the disturbance is assumed in the set

$$\mathcal{D} = \{d \in \mathbb{R}^r \ : \ ||d||_2/N \le d_{\max}\}, \tag{6}$$

---

[1]According to K. Popper [45], a theory can only be *falsified* or *invalidated* with certainty, never validated. This is because future data (that might (in)validate the theory) are not accessible. This applies also to dynamical models which mimic physical data.
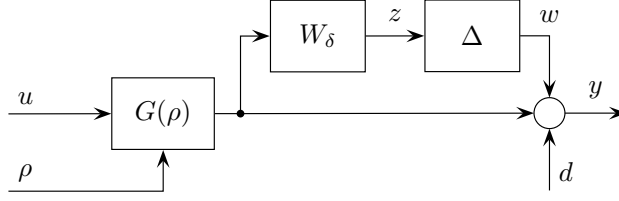
Figure 1: Model (in)validation setup.

with $||d||_2 = \sqrt{\sum_0^N d(t_k)^T d(t_k)}$. This framework is adequate for robust controller design methods, such as: $\mathcal{H}_\infty$ optimal control, LPV or switched (LTI) LPV control. The theory for model (in)validation has been initially proposed in [34] and then extended to LPV systems in [46].

The relation among signals corresponding to the system description in Figure 1 can be expressed as:

$$
\begin{aligned}
T_z &= T_{W_\delta} T_G T_u, \\
T_y &= T_w + T_G T_u + T_d, \\
T_w &= T_\Delta T_z,
\end{aligned}
\tag{7}
$$

where $T_{W_\delta}$, $T_G$ and $T_\Delta$ are the Toeplitz matrices associated with convolution kernels of $G(\rho)$, $W_\delta$ and $\Delta$, respectively. The symbols $T_z$, $T_u$, $T_y$, $T_d$ and $T_w$ are the Toeplitz matrices associated to the sequences $\mathbf{u}$, $\mathbf{y}$, $\mathbf{d}$, and $\mathbf{w}$, respectively. The bold letters denote the respective truncated version of the signals as follows: $\mathbf{x} = [x_0^T \ldots x_{N-1}^T]$ (see [34, 46] for more details).

The model set given by $\mathcal{G}$ is (in)validated against experimental data provided by vectors $\mathbf{u}$, $\mathbf{y}$, and $\boldsymbol{\rho}$, if there exist vectors $\mathbf{w}$ and $\mathbf{d}$ satisfying constraints (4) and (6). This is defined as consistency, and for the model, uncertainty and noise sets are *not* invalidated by the existing data. The (in)validation of the model in Figure 1 can be expressed as a convex optimization problem. More concretely, the measures of $u(t_k)$, $y(t_k)$ and $\rho(t_k)$ with $k = 0, \ldots, N-1$ are consistent with the model in Figure 1 if the following optimization problem is feasible:

$$
\underset{\mathbf{d}, \mathbf{w}}{\text{minimize}} \quad \gamma
\tag{8a}
$$

$$
\text{subject to} \quad \begin{bmatrix} T_u^T (T_{W_\delta} T_G)^T T_{W_\delta} T_G T_u & T_w^T(\mathbf{w}) \\ T_w(\mathbf{w}) & \gamma^2 I \end{bmatrix} > 0,
\tag{8b}
$$

$$
\begin{bmatrix} d_{\max}^2 & \mathbf{d}^T \\ \mathbf{d} & I \end{bmatrix} > 0
\tag{8c}
$$

where $\mathbf{d} = \mathbf{y} - \mathbf{w} - T_G \mathbf{u}$.

## 3. LPV model invalidation of *in-silico* patients

In this section, the model (in)validation tools presented in Section 2.2 are used to test consistency of the LPV model presented in Section 2.1 against the *experimental* noiseless evidence obtained from the UVA/Padova simulator. Thus, the output noise bound is set at a very small value and the optimization

5

problem (8) is solved to determine the minimum uncertainty bound $\gamma$. The tools used for optimization using the Linear Matrix Inequality (LMI) framework are SeDuMi [47] and Yalmip [48].

The experimental data sets $[u(t_k), y(t_k), \rho(t_k)]$ were generated by extensive simulations using two types of realistic insulin profiles. The first one represents a correction insulin bolus of the form:

$$u(t) = \begin{cases} \theta/T_s, & \text{if } t_0 \leq t \leq t_0 + T_s, \\ 0 & \text{otherwise,} \end{cases} \tag{9}$$

where $T_s = 5$ minutes is the sampling time and $\theta$ a random number in the range $[0.5, 1.5]$ U. The second profile is a basal insulin modulation signal:

$$u(t) = \sum_{k=1}^{n} (1 + \zeta) u_{\text{b}} \phi(kT_p) \tag{10}$$

where $u_{\text{b}}$ is the basal infusion rate, $\zeta$ is a random number in the range $[-0.5, 0.5]$, $\phi(t)$ is a pulse signal of width $T_p = 60$ minutes and $nT_p$ is the total simulation time. This signal mimics the modulation of the basal insulin infusion rate during a closed-loop test, as the one that will illustrate these results in Section 4.

The difference between the *experiment* and the model during the invalidation process covers dynamic and/or parametric uncertainties. The first one involves the different dynamical behaviors of the system when moving from one glucose value to another. Specifically, this represents different LTI models moving over a nonlinear dynamical surface. In addition, an important type of parameter variation that has relevance in this problem is the uncertainty in $S_I$, which is related to the well-known intra-patient variations. In order to consider this variability, seven versions of each *in-silico* adult of the distribution version of the UVA/Padova simulator were generated by affecting the nominal insulin sensitivity ($S_{I,\text{nom}}$) with factor values in the set $\{0.5, \ 0.7, \ 0.9, \ 1, \ 1.1, \ 1.3, \ 1.5\}$. These values were selected according to results presented in [49]. Variations in $S_I$ were implemented as changes in the model parameters $V_{mx}$ and $k_{p3}$ that represent the peripheral and hepatic insulin sensitivity, respectively (see [5] for a complete description of model equations).

To collect sufficient representative information of each *in-silico* adult, they were excited with three signals of the form (9) and five of the form (10). As an example, Figure 2 shows the excitation signals and glucose evolution corresponding to the experiments performed on Adult #001 with sensitivity $S_{I,\text{nom}}$. The upper plots correspond to the input signals and the bottom plots correspond to the glucose responses obtained with the UVA/Padova simulator and the LPV model. Bearing in mind that different insulin sensitivities are used, effects of insulin modulations in a wider range are considered, at least in nominal conditions. For example, a 1.5 U bolus for $S_I = 1.5 \ S_{I,\text{nom}}$ would be similar to a lower bolus with the nominal $S_I$, or a larger bolus with a lower $S_I$. Moreover, the range of insulin profiles used in this work was limited in order to guarantee that the glucose traces, in all cases, remain in the simulator's domain of validity, i.e., $[40, 400]$ mg/dl.

The model (in)validation discussed above requires a discrete model. Therefore, the LPV model proposed in Section 2.1 was transformed into:

$$x(t_{k+1}) = A_d[p_1(t_k)] \ x(t_k) + B_d \ u(t_k),$$
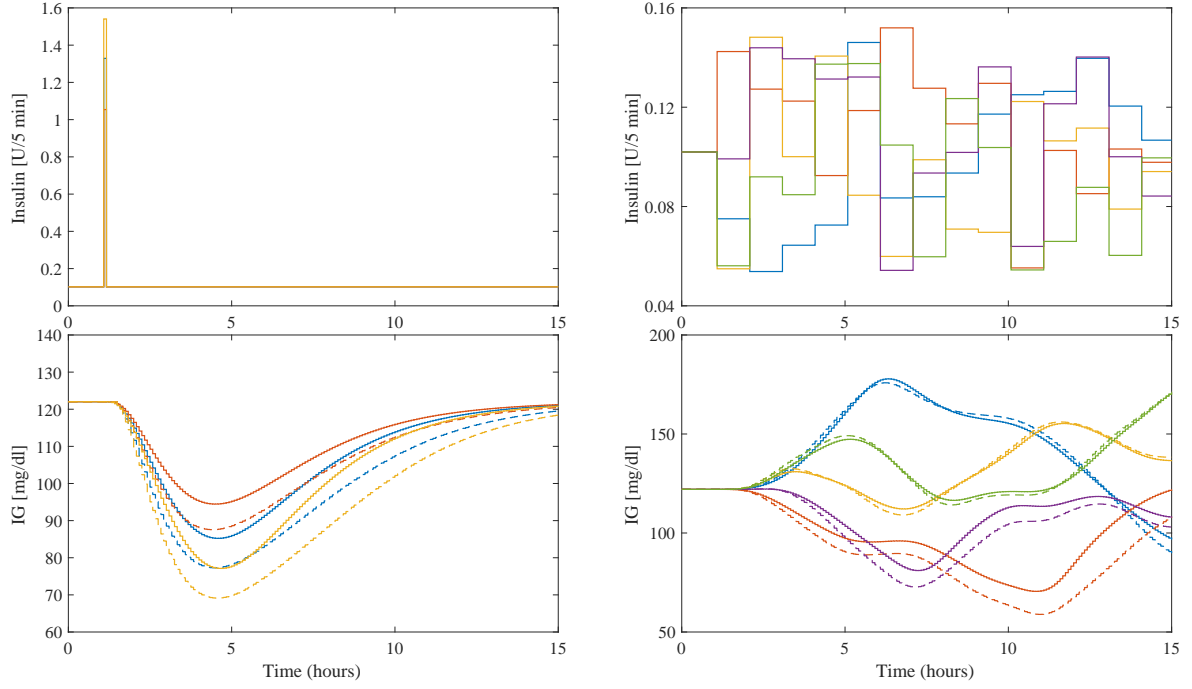$$y(t_k) = C_d \ x(t_k),$$

6

Figure 2: *In-silico* experimental results with the insulin bolus test signal (left) and the basal insulin modulation test signal (right) applied to Adult #001 with sensitivity $S_{I,\text{nom}}$. Insulin infusion rate (upper) and glucose response (lower) obtained with UVA/Padova simulator (solid line) with LPV model (dashed line).

where

$$A_d[p_1(t_k)] = \begin{bmatrix} I + T_s A[p_1(t_k)] & 0 \\ B_e C & A_e \end{bmatrix}, \qquad B_d = \begin{bmatrix} T_s B_e \\ 0 \end{bmatrix}, \qquad C_d = \begin{bmatrix} 0 & C_e \end{bmatrix},$$

$$A_e = \begin{bmatrix} 0 & 0 & 0 \\ 1 & 0 & 0 \\ 0 & 1 & 0 \end{bmatrix}, \qquad B_e = \begin{bmatrix} 1 \\ 0 \\ 0 \end{bmatrix}, \qquad C_e = \begin{bmatrix} 0 & 0 & 1 \end{bmatrix}.$$

The noise signal set was defined in (6) with $d_{\max} = 0.05$, and the uncertainty weight in (4) as:

$$W_\delta(s) = 0.2 \, \frac{500s + 1}{50s + 1} \tag{11}$$

In model (in)validation, the differences between the experimental data and the model are "explained" by the model uncertainty $\Delta$ and a noise set bounded by $d_{\max}$ mg/dl. Here, noise-free results from the UVA/Padova simulator have been used as "experimental data". This is the reason for choosing such a small noise bound $d_{\max}$. In addition the noise set serves to consider noisy data, but this bound has no implications in the control design. In next section more realistic noisy scenarios are considered to test the proposed robust controller, which does not affect the validity of the uncertain model.

Hence, all differences between the model and the experiment are attributed to non-linearities and un-modeled phenomena, which can affect stability and performance. Here $W_\delta(s)$ is a high-pass filter because above a certain frequency, uncertainty impedes the stabilization of the closed-loop. The only designer's
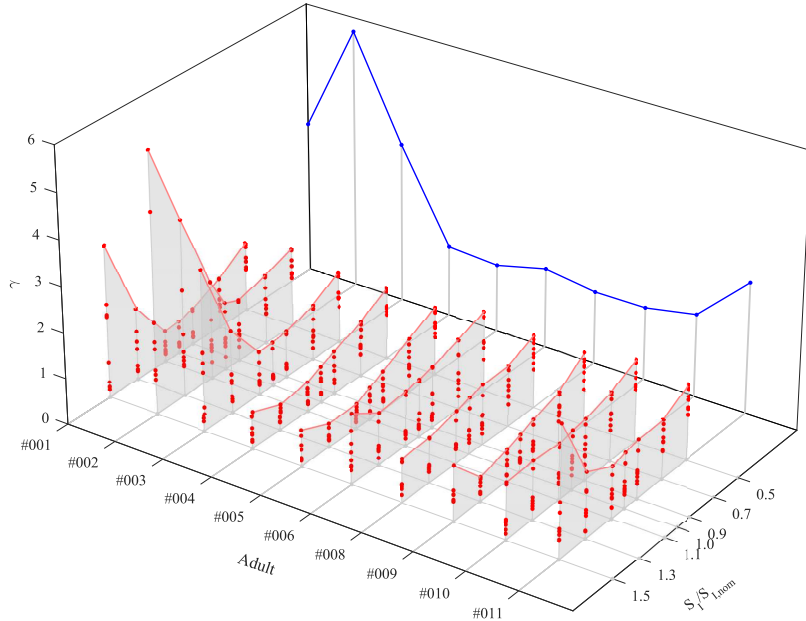
Figure 3: Summary of the uncertainty bounds $\gamma$ obtained for the eight test signals applied to each *in-silico* adult with seven different $S_I$. The blue line indicates the worst-case uncertainty bound $\gamma_{ws}$

choice is the maximum achievable closed-loop bandwidth ($2 \times 10^{-3}$ rad/min in eqn. (11)) which was chosen according to the *a priori* knowledge on the system, in order to cover the nominal model's dynamics. Its magnitude depends on the *experimental* knowledge of the system, and is computed as an uncertainty bound $\gamma$ in the set (5) which scales $W_\delta(s)$ during the controller design. The magnitude depends on the proposed uncertain model, and in general can be reduced if a more complex model set is used, e.g., higher order. Therefore, the 20% uncertainty that $W_\delta(s)$ has at low frequencies is only a starting point, since the actual magnitude is computed by means of the (in)validation procedure.

The uncertainty bounds $\gamma$ obtained after solving the optimization problem (8) for each data set and for each *in-silico* adult are summarized in Figure 3. Adult #007 has been excluded because its TDI is not compatible with its $S_I$. In addition, the invalidation tests performed on this subject have shown a clear inconsistency between model and data, turning it into an outlier of the set in terms of model uncertainty. The red dots indicate the $\gamma$ for each test and the red line the worst case bound for each combination of subject-$S_I$. The blue line indicates the worst-case uncertainty bound $\gamma_{ws}$ for each adult. This last bound can be used in LPV synthesis tools for the controller design by scaling the uncertainty weight as $\gamma_{ws}W_\delta(s)$. The corresponding values obtained in the model (in)validation are listed in Table 1.

## 4. Switched-LPV robust controller design

The use of the set of models obtained previously is illustrated in this section designing a switched-LPV controller. To this end, each subject is represented by the set of models computed in Section 3, and extending the ideas in [11, 16], a (robust) switched LPV controller is synthesized based on this set. This

| $S_I/S_{I,nom}$ | Adult | | | | | | | | | |
|---|---|---|---|---|---|---|---|---|---|---|
| | #001 | #002 | #003 | #004 | #005 | #006 | #008 | #009 | #010 | #011 |
| 0.5 | 1.524 | 1.735 | 1.555 | 1.560 | 1.484 | 1.754 | 1.596 | 1.598 | 1.808 | 1.637 |
| 0.7 | 1.093 | 1.515 | 1.194 | 1.190 | 1.185 | 1.530 | 1.326 | 1.124 | 1.502 | 1.298 |
| 0.9 | 0.791 | 1.350 | 1.015 | 0.934 | 0.858 | 1.332 | 1.318 | 0.949 | 1.344 | 1.282 |
| 1.0 | 0.698 | 1.479 | 0.958 | 0.787 | 0.696 | 1.256 | 1.238 | 0.822 | 1.301 | 1.208 |
| 1.1 | 0.681 | 2.131 | 0.948 | 0.646 | 0.540 | 1.196 | 1.147 | 0.700 | 1.218 | 1.128 |
| 1.3 | 1.566 | 3.859 | 1.801 | 0.552 | 0.523 | 1.135 | 0.989 | 0.526 | 1.276 | 1.431 |
| 1.5 | 3.327 | 5.694 | 3.510 | 0.798 | 0.791 | 1.528 | 0.940 | 1.197 | 1.231 | 2.864 |
| $\gamma_{ws}$ | 3.327 | 5.694 | 3.510 | 1.560 | 1.484 | 1.754 | 1.596 | 1.598 | 1.808 | 2.864 |

Table 1: Uncertainty bounds for each *in-silico* adult and each variation in $S_I$. The worst-case bounds are $\gamma_{ws}$.

design switches between two LPV controllers: $K_1(\rho)$ that is conservative and performs slight changes on the basal insulin infusion rate, and $K_2(\rho)$ that is more aggressive and is triggered at meal times.

The design of LPV controllers follows similar procedures as $\mathcal{H}_\infty$ optimal control, but for time-varying systems. The controller is computed solving a convex optimization problem aimed at minimizing the $\mathcal{L}_2$ gain of the mapping from a generic disturbance $w$ to an output $z$, i.e., minimizing a scalar $\eta > 0$ such that

$$\|z\|_2 < \eta \|w\|_2,$$

where $\|x\|_2 = \sqrt{\int_0^\infty x^T(t)x(t)\,dt}$. Therefore, the design involves selecting $w$ and $z$ according to the control specifications. In the case of the AP, the structure of weights and signals are illustrated in Figure 4. In this framework, a controller designed to cope with an uncertain system represented by a set of models, works properly when nominal performance and robust stability are satisfied.

Here, nominal performance pertains the minimization of two selected variables under a *set* of possible perturbations $r$. Thus, it is achieved by solving the minimization of a gain $\alpha > 0$ for all $r$ bounded in $\mathcal{L}_2$ such that:

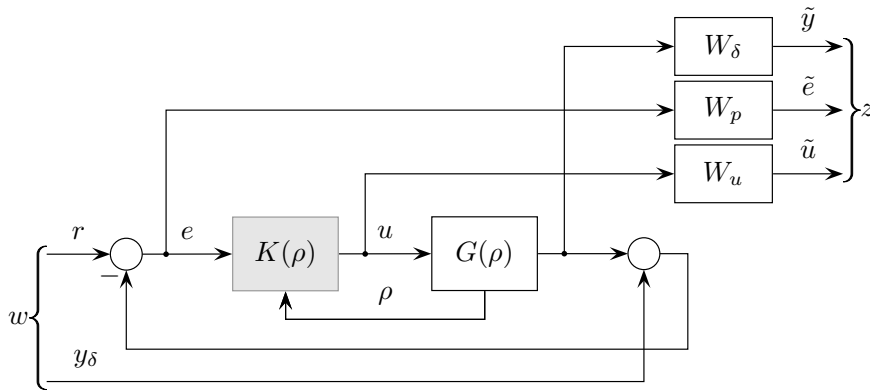$$\left\| \begin{bmatrix} \tilde{e} \\ \tilde{u} \end{bmatrix} \right\|_2 < \alpha \|r\|_2, \tag{12}$$



Figure 4: Robust LPV control design setup.

9

| Adult | #001 | #002 | #003 | #004 | #005 | #006 | #008 | #009 | #010 | #011 |
|-------|------|------|------|------|------|------|------|------|------|------|
| $\gamma_{ws}$ | 3.327 | 5.694 | 3.510 | 1.560 | 1.484 | 1.754 | 1.596 | 1.598 | 1.808 | 2.864 |
| $k_e$ | 0.023 | 0.016 | 0.023 | 0.045 | 0.050 | 0.043 | 0.047 | 0.046 | 0.041 | 0.027 |
| $\eta_1$ | 1.081 | 1.042 | 1.122 | 1.281 | 1.388 | 1.474 | 1.423 | 1.301 | 1.311 | 1.129 |
| $\beta_1$ | 0.949 | 0.982 | 0.965 | 0.861 | 0.849 | 0.812 | 0.835 | 0.887 | 0.878 | 0.961 |
| $\eta_2$ | 1.014 | 1.012 | 1.039 | 1.078 | 1.130 | 1.142 | 1.138 | 1.101 | 1.100 | 1.045 |
| $\beta_2$ | 0.982 | 0.988 | 1.005 | 0.975 | 0.993 | 0.999 | 0.999 | 0.997 | 1.001 | 1.005 |

Table 2: Results corresponding to the LPV robust controller design for each *in silico* adult.

where $\tilde{e}$ and $\tilde{u}$ are obtained after weighting the glucose error $e$ and the control action $u$ (insulin infusion) with the following weights:

$$W_p(s) = \frac{k_e}{10} \frac{10s + 1}{5000s + 1}, \tag{13}$$

$$W_u = k_{u,j}, \tag{14}$$

respectively. The variable $j \in \{1, 2\}$ corresponds to the controller index in the switching strategy. Weight $W_p(s)$ penalizes glucose deviations from the basal value (around 120 mg/dl [5]) and weight $W_u$ penalizes large changes in the insulin injection. Both weights are the only controller tunning parameters, and are selected according to the designer's priorities. In this work, these performance weights have been selected in order to prioritize avoidance of hypoglycemia rather than the lack of hyperglycemia, considering the short and long term consequences of each state.

Robust stability consists in guaranteeing that the controller stabilizes the closed-loop system for any possible model in the set (4), and therefore stabilizes the underlying uncertain dynamics. To this end, the controller must be computed in order to ensure $\beta < 1$ where

$$\|\tilde{y}\|_2 < \beta \, \|y_\delta\|_2.$$

Variable $\tilde{y}$ is obtained after weighting $y$ with the uncertainty dynamics (11) affected by the worst-case bound $\gamma_{ws}$ corresponding to the particular subject, i.e., $\gamma_{ws} W_\delta(s)$.

Table 2 summarizes the controller design results. For all subjects, the parameter in $W_u$ was set as $k_{u,1} = 0.5$ and $k_{u,2} = 0.07$. Note that $k_{u,2}$ is significantly smaller than $k_{u,1}$, and therefore provides a lower weight on the control variable which in turn produces a more aggressive controller (higher insulin infusion at meal times). Parameter $k_e$ was adjusted for each patient in order to ensure the robust stability condition $\beta < 1$. Notice that by norm properties $\beta \leq \eta$, nevertheless forcing $\eta < 1$ might result in a very conservative controller design. For this reason, the parameter $k_e$ for each patient was selected according to the gain $\beta$. From Table 2 it is clear that those subjects with higher uncertainty bound $\gamma_{ws}$ require lower values of $k_e$, which implies a lower performance, i.e., a worst glucose regulation.

Closed-loop simulations were performed considering the following conditions: (i) the UVA/Padova distribution simulator; (ii) a meal of 70 g of CHO is ingested at hour 7; (iii) the aggressive controller is triggered exactly at meal time and commands the insulin infusion; (iv) one hour after meal time, the conservative controller automatically takes over the insulin delivery; and (v) a CGM sensor and an insulin
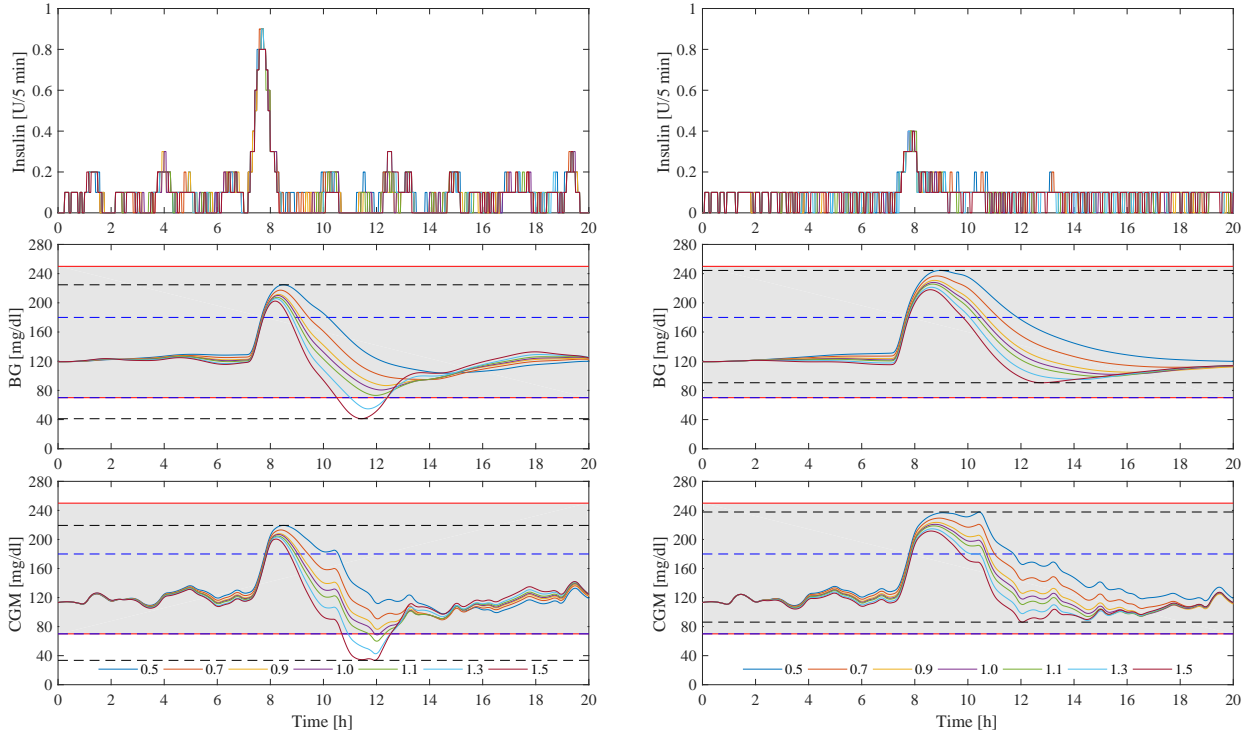
Figure 5: Closed-loop responses for one *in-silico* adult to a meal of 70 g of CHO at the hour 7, using the nominal controller (left) and the robust controller (right). Seven variations of $S_I$ are considered and the same CGM noise is applied in all cases for comparison purposes. The continuous red lines represent the limits of the 70-250 mg/dl range, the dashed blue lines indicate the limits of the 70-180 mg/dl range, and the dashed black lines indicate the minimum and maximum glucose values.

pump with a delivery resolution of 0.1 U. It is worth clarifying that meal announcement is made only for triggering the aggressive controller, but no information regarding the carbohydrate amount is required by the controller, and therefore, no pre-meal insulin boluses are infused.

Figure 5 presents simulations of the closed-loop system for one *in-silico* adult, where each line corresponds to a particular subject's $S_I$ indicated in Section 3. Plots on the right correspond to the closed-loop system with the robust controller designed as mentioned in this section. Plots on the left show the closed-loop responses with a nominal controller, i.e., a controller designed considering only the performance objective (12) and not the model set (4) (model uncertainty is excluded) with the same $k_{u,j}$ and $k_e = 1$. Comparing both responses, it can be observed that the nominal controller is more aggressive than the robust one, applying higher insulin doses. This result is suitable for $S_I$ values close to $S_{I,nom}$, but not when the $S_I$ is far from the nominal value. This is clear in the case of a more sensitive value as $S_I = 1.5S_{I,nom}$ in which a significant postprandial glucose drop can be observed (minimum blood glucose around 40 mg/dl). On the other hand, the robust controller is more conservative, using lower insulin values, but produces a more uniform response for all $S_I$ cases (minimum blood glucose around 90 mg/dl). These results are reasonable from the point of view of robust control theory: a controller that aims for a particular (nominal) model representation of the patient will show its worst performance when the model does not match the actual patient. Instead, a robust controller that should manage a set of models (a more realistic representation of the patient) already considers possible uncertainties in both model dynamics and parameters, and therefore
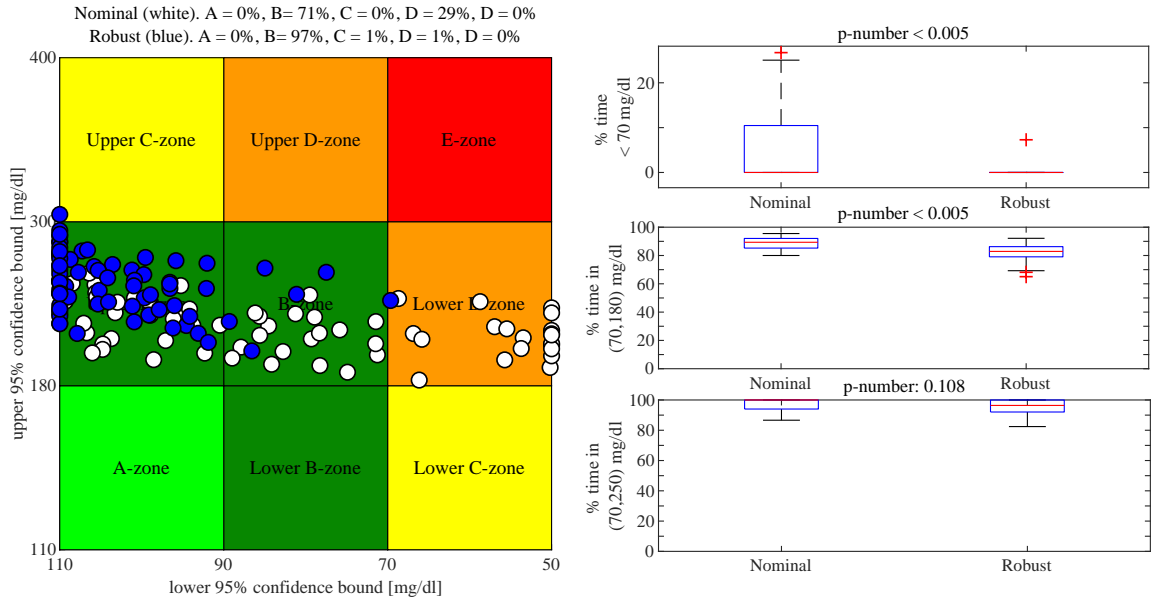
11

Figure 6: Left: CVGA plots of the closed-loop responses of all *in-silico* adults and their $S_I$ variations for the nominal (white) and the robust controllers (blue). Right: Time-in-range plots.

will perform at its best in general, although in a more conservative fashion.

Figure 6 provides the closed-loop results for all *in-silico* adults in a CVGA (left) and time-in-range (right) plots. Time-in-range results are computed from the meal time to the end of the simulation. A comparison is made between the nominal and robust controller designs over all subjects, including their $S_I$ variations. From the CVGA plot, the nominal controller presents a higher number of subjects in the lower D-zone (nominal: 29%, robust: 1%), indicating risk of hypoglycemia. Instead, the robust controller is located in the B- and upper B-zones, achieving a significant reduction in hypoglycemic events, compared to the nominal one. This situation is also shown in the time-in-range plot, where a significant reduction of time in hypoglycemia ($< 70$ mg/dl) is achieved (nominal: 2.67% vs. robust: 0.05%, $p < 0.05$), without significantly reducing the percentage of time in range [70, 250] mg/dl (nominal: 96.85% vs. robust: 95.48%, $p = 0.108$). Although there is a significant reduction in percentage of time in range [70, 180] mg/dl when the robust controller is used (nominal: 88.75% vs. robust: 82.19%, $p < 0.05$), time in range achieved with the robust controller is still acceptable. Hyperglycemic behavior arises as a consequence of the conservative tendency of the robust controller, coming from a large uncertainty bound, and therefore, it can be reduced by further refining of the uncertainty bounds by means of more (and better) information of each patient.

## 5. Conclusions and Future research

In this work, an LPV invalidation technique has been applied to a control-oriented LPV model in order to expand the insulin-glucose description to a set of LPV models. This set is instrumental for robust controller design, which in this work has been carried out by a switched LPV procedure. The controller design based on this model set has proved useful when dynamic and parametric uncertainties appear in the problem. An illustrative example presents a robust controller that copes with uncertainties in the nonlinear dynamics

12

(changes in the glucose values) and variations in $S_I$, as compared to a nominal design.

In terms of future work, an important issue to be solved next is how to apply this modeling strategy from real clinical data in a minimally invasive way. There are several alternatives, but the one that will be explored is the use of the patient's daily data recorded by the CGM and pump to invalidate the LPV model and obtain the patient's particular model set. In this way a robust controller can be designed, and tested clinically on the same subject. Using clinical data, which could have lower excitability, will not affect the procedure, since the difference between the clinical data and the model output comes from the patient and the model set obtained (which now represents this patient) is the one to be controlled.

Additionally, there are different approaches to account for parameter variations in the controller design stage. One is to cover them with dynamic uncertainty, as has been presented here, selecting a single uncertainty bound for each patient. Another is to select an LPV uncertainty weight for the design that accounts for its variation with the subject's $S_I$. In the latter approach, a real-time estimation of $S_I$ like the one developed in [50] from CGM and insulin pump data could be used. A third approach would be to formalize intra-patient variations in an LPV model that includes this variation in a way that allows for the real-time estimation of patients $S_I$ daily variability. The last two approaches could increase the performance of the resulting controller.

## 6. Acknowledgements

## References

[1] A. Chait, K. E. Bornfeldt, Diabetes and atherosclerosis: Is there a role for hyperglycemia?, J. Lipid Res. 50 (2009) S335–S339.

[2] G. M. Steil, A. E. Panteleon, K. Rebrin, Closed-loop insulin delivery-the path to physiological glucose control, Adv. Drug Deliv. Rev. 56 (2) (2004) 125–144.

[3] B. P. Kovatchev, M. Breton, C. Dalla Man, C. Cobelli, In silico model and computer simulation environment approximating the human glucose/insulin utilization, Food and Drug Administration Master File MAF 1521.

[4] B. P. Kovatchev, M. Breton, C. Dalla Man, C. Cobelli, In silico preclinical trials: A proof of concept in closed-loop control of type 1 diabetes, J. Diabetes Sci. Technol. 3 (1) (2009) 44–55.

[5] C. Dalla Man, F. Micheletto, D. Lv, M. Breton, B. P. Kovatchev, C. Cobelli, The UVA/PADOVA type 1 diabetes simulator: New features, J. Diabetes Sci. Technol. 8 (1) (2014) 26–34.

[6] K. van Heusden, E. Dassau, H. C. Zisser, D. E. Seborg, F. J. Doyle III, Control-relevant models for glucose control using *a priori* patient characteristics, IEEE Trans. Biomed. Eng. 59 (7) (2012) 1839–1849.

[7] P. Soru, G. De Nicolao, C. Toffanin, C. Dalla Man, C. Cobelli, L. Magni, on behalf of the AP@home consortium, MPC based Artificial Pancreas : Strategies for individualization and meal compensation, Annu. Rev. Control 36 (2012) 118–128.

[8] S. D. Patek, L. Magni, E. Dassau, C. Hughes-Karvetski, C. Toffanin, G. De Nicolao, S. Del Favero, M. Breton, C. Dalla Man, E. Renard, H. Zisser, F. J. Doyle III, C. Cobelli, B. P. Kovatchev, International Artificial Pancreas (iAP) Study Group, Modular closed-loop control of diabetes, IEEE Trans. Biomed. Eng 59 (11) (2012) 2986–2999.

[9] J. Lee, E. Dassau, D. Seborg, F. J. Doyle III, Model-based personalization scheme of an artificial pancreas for type 1 diabetes applications, in: American Control Conference (ACC), Washington, DC, USA, 2013, pp. 2911–2916.

[10] K. Turksoy, L. Quinn, E. Littlejohn, A. Cinar, Multivariable adaptive identification and control for artificial pancreas systems, IEEE Trans. Biomed. Eng. 61 (3) (2014) 883–891.

[11] P. Colmegna, R. S. Sánchez-Peña, R. Gondhalekar, E. Dassau, F. J. Doyle III, Switched LPV glucose control in type 1 diabetes, IEEE Trans. Biomed. Eng. 63 (6) (2016) 1192–1200.

[12] R. Gondhalekar, E. Dassau, F. J. Doyle III, Periodic zone-MPC with asymmetric costs for outpatient-ready safety of an artificial pancreas to treat type 1 diabetes, Automatica 71 (9) (2016) 237–246.

[13] M. Messori, C. Toffanin, S. D. Favero, G. De Nicolao, C. Cobelli, L. Magni, Model individualization for artificial pancreas, Comput. Meth. Prog. Bio. (2016). DOI: 10.1016/j.cmpb.2016.06.006.

[14] P. Colmegna, F. Garelli, H. D. Battista, R. Sánchez-Peña, Automatic regulatory control in type 1 diabetes without carbohydrate counting, Control Eng. Pract. 74 (2018) 22–32.

[15] M. Messori, G. P. Incremona, C. Cobelli, L. Magni, Individualized model predictive control for the artificial pancreas: In silico evaluation of closed-loop glucose control, IEEE Contr. Syst. Mag. 38 (1) (2018) 86–104.

[16] P. Colmegna, R. Sánchez-Peña, R. Gondhalekar, Linear parameter-varying model to design control laws for an artificial pancreas, Biomed. Signal Process. Control 40 (2018) 204–213.

[17] R. Sánchez-Peña, F. Bianchi, Model selection: from LTI to switched-LPV, in: American Control Conference (ACC), Montreal, Canada, 2012, pp. 1561–1566.

[18] P. G. Fabietti, V. Canonico, M. O. Federici, M. M. Benedetti, E. Sarti, Control oriented model of insulin and glucose dynamics in type 1 diabetics, Med. Biol. Eng. Comput. 44 (1-2) (2006) 69–78.

[19] L. Kovács, B. Kulcsár, J. Bokor, Z. Benyó, LPV fault detection of glucose-insulin system, in: 14th Mediterranean Conference on Control and Automation, Ancona, Italy, 2006, pp. 1–5.

[20] P. Szalay, G. Eigner, L. A. Kovács, Linear matrix inequality-based robust controller design for type-1 diabetes model, in: 19th IFAC World Congress, Cape Town, South Africa, 2014, pp. 9247–9252.

[21] J. Bondia, S. Romero-Vivo, B. Ricarte, J. L. Diez, Insulin estimation and prediction: A review of the estimation and prediction of subcutaneous insulin pharmacokinetics in closed-loop glucose control, IEEE Contr. Syst. Mag. 38 (1) (2018) 47–66.

[22] A. J. Laguna, P. Rossetti, F. J. Ampudia-Blasco, J. Vehí, J. Bondia, Identification of intra-patient variability in the postprandial response of patients with type 1 diabetes, Biomed. Signal Proces. 12 (1) (2014) 39–46.

[23] D. de Pereda, S. Romero-Vivo, B. Ricarte, J. Bondia, On the prediction of glucose concentration under intra-patient variability in type 1 diabetes: A monotone systems approach, Comput. Meth. Prog. Bio. 108 (3) (2012) 993–1001.

[24] M. García-Jaramillo, R. Calm, J. Bondia, J. Vehí, Prediction of postprandial blood glucose under uncertainty and intra-patient variability in type 1 diabetes: A comparative study of three interval models, Comput. Meth. Prog. Bio. 108 (1) (2012) 224–233.

[25] E. Ruiz-Velázquez, R. Femat, D. Campos-Delgado, Blood glucose control for type I diabetes mellitus: A robust tracking $\mathcal{H}_\infty$ problem, Control Engineering Practice 12 (2004) 1179–1195.

[26] R. S. Parker, F. J. Doyle III, J. H. Ward, N. A. Peppas, Robust $\mathcal{H}_\infty$ glucose control in diabetes using a physiological model, A.I.Ch.E. Journal 46 (12) (2000) 2537–2549.

[27] P. Colmegna, R. Sánchez-Peña, R. Gondhalekar, E. Dassau, F. J. Doyle III, Reducing risks in type 1 diabetes using $\mathcal{H}_\infty$ control, IEEE Trans. Biomed. Eng. 61 (12) (2014) 2939–2947.

[28] L. Kovács, B. Kulcsár, LPV modeling of type I diabetes mellitus, in: 8th International Symposium of Hungarian Researchers, 2007, pp. 163–173.

[29] L. Kovács, B. Kulcsár, J. Bokor, Z. Benyó, Model-based nonlinear optimal blood glucose control of Type I diabetes patients, in: 30th Annual International IEEE EMBS Conference, Vancouver, Canada, 2008, pp. 1607–1610.

[30] L. Kovács, B. Benyó, J. Bokor, Z. Benyó, Induced $\mathcal{L}_2$-norm minimization of glucose-insulin system for type i diabetic patients, Computer Methods and Programs in Biomedicine 102 (2011) 105–118.

[31] P. Colmegna, R. Sánchez-Peña, R. Gondhalekar, E. Dassau, F. J. Doyle III, Reducing glucose variability due to meals and postprandial exercise in T1DM using switched LPV control: In silico studies, J. Diabetes Sci. Technol. 10 (3) (2016) 744–753.

[32] P. Herrero, Z. Chen, J. Bondia, P. Georgiou, C. Toumazou, Interval-based model predictive control for an artificial pancreas, in: Diabetes Technology & Therapeutics, Vol. 17, 2015.

[33] S. Schaller, J. Lippert, L. Schaupp, T. R. Pieber, A. Schuppert, T. Eissing, Robust PBPK/PD-based model predictive control of blood glucose, IEEE Transactions on Biomedical Engineering 63 (7) (2016) 1492–1504.

[34] R. Smith, Model validation for uncertain systems, Ph.D. thesis, California Institute of Technology (1990).

[35] R. Smith, G. Dullerud, S. Rangan, K. Poolla, Model validation for dynamically uncertain systems, Math. Comp. Model. Dyn 3 (1) (1997) 43–58.

[36] P. Colmegna, R. Sánchez-Peña, R. Gondhalekar, Control-oriented linear parameter-varying model for glucose control in type 1 diabetes, in: IEEE Multi-Conference on Systems and Control, Buenos Aires, Argentina, 2016, pp. 410–415.

14

[37] J. Walsh, R. Roberts, Pumping Insulin, 4th Edition, Torrey Pines Press, San Diego, CA, 2006.

[38] R. Sánchez-Peña, A. Ghersin, LPV control of glucose for type 1 diabetes, in: IEEE EMBS (Ed.), 32nd Annual International Conference, Buenos Aires, Argentina, 2010, pp. 680–683.

[39] L. Kovács, B. Kulcsár, LPV modeling of type I diabetes mellitus, in: 8th International Symposium of Hungarian Researchers, Budapest, Hungary, 2007, pp. 163–173.

[40] L. Kovács, B. Kulcsár, J. Bokor, Z. Benyó, Model-based nonlinear optimal blood glucose control of type I diabetes patients, in: 30th Annual International IEEE EMBS Conference, Vancouver, BC, Canada, 2008, pp. 1607–1610.

[41] L. Kovács, B. Benyó, J. Bokor, Z. Benyó, Induced $\mathcal{L}_2$-norm minimization of glucose-insulin system for type I diabetic patients, Comput. Meth. Progr. Bio. 102 (2) (2011) 105–118.

[42] R. N. Bergman, Y. Ider, C. Bowden, C. Cobelli, Quantitative estimation of insulin sensitivity, Am. J. Physiol. 236 (6) (1979) E667–677.

[43] J. T. Sorensen, A physiologic model of glucose metabolism in man and its use to design and asses improved insulin therapies for diabetes, Ph.D. thesis, Massachusetts Institute of Technology, Cambridge, MA, USA (1985).

[44] R. Hovorka, F. Shojaee-Moradie, P. Carroll, L. Chassin, I. Gowrie, N. Jackson, R. Tudor, A. Umpleby, R. Jones, Partitioning glucose distribution/transport, disposal, and endogenous production during IVGTT, Am. J. Physiol. Endocrinol. Metab. 282 (5) (2002) E992–1007.

[45] K. R. Popper, Conjectures and Refutations: The Growth of Scientific Knowledge, London: Routledge, 1963.

[46] M. Sznaier, M. C. Mazzaro, An LMI approach to control-oriented identification and model (in)validation of LPV systems, IEEE Trans Automat Contr 48 (9) (2003) 1619–1624.

[47] J. F. Sturm, Using SeDuMi 1.02, a MATLAB toolbox for optimization over symmetric cones, Optimization Methods and Software 11 (1-4) (1999) 625–653.

[48] J. Löfberg, YALMIP: A toolbox for modeling and optimization in MATLAB, in: In Proceedings of the CACSD Conference, Taipei, Taiwan, 2004.

[49] L. Hinshaw, C. Dalla Man, D. K. Nandy, A. Saad, A. E. Bharucha, J. A. Levine, R. A. Rizza, R. Basu, R. E. Carter, C. Cobelli, et al., Diurnal pattern of insulin action in type 1 diabetes: implications for a closed loop system, Diabetes (2013) 2223–2229.

[50] M. Schiavon, C. Dalla Man, Y. C. Kudva, A. Basu, C. Cobelli, Quantitative estimation of insulin sensitivity in type 1 diabetic subjects wearing a sensor augmented insulin pump, Diabetes care 37 (5) (2013) 39–49.